

# Fluorescence and NMR Characterization and Biomolecule Entrapment Studies of Sol–Gel-Derived Organic–Inorganic Composite Materials Formed by Sonication of Precursors

John D. Brennan,<sup>\*,†</sup> J. Stephen Hartman,<sup>‡</sup> Elizabeth I. Ilnicki,<sup>‡</sup> and Michael Rakic<sup>†</sup>

Department of Chemistry, McMaster University, Hamilton, Ontario, L8S 4M1, Canada, and  
Department of Chemistry, Brock University, St. Catharines, Ontario, L2S 3A1, Canada

Received January 28, 1999

Optically clear sol–gel-derived organic–inorganic hybrid materials were prepared by a sonication method suitable for entrapment of biological compounds. Sonication at pH 2.5 hydrolyzed mixtures of tetraethyl orthosilicate (TEOS) and one of the organosilanes methyltriethoxysilane (MTES), propyltrimethoxysilane (PTMS), or dimethyldimethoxysilane (DMDMS). Buffer solutions containing the fluorescent probes 7-azaindole or prodan, or the proteins human serum albumin (HSA) or lipase, were then added to promote gelation and the resulting materials were aged at 4 °C over several months. The optical clarity, hardness, and degree of cracking were examined, in conjunction with solid-state <sup>29</sup>Si and <sup>13</sup>C NMR of the materials and fluorescence spectra of the entrapped probes. These studies revealed that MTES can be added to TEOS up to a level of 20% (v/v) with retention of good physical characteristics, thus allowing control over the hydrophobicity and cross-linking within the matrix. Materials with more than 20% MTES, or incorporating PTMS or DMDMS at levels above 5%, showed significantly poorer physical characteristics, indicating phase separation. Proteins entrapped into these hybrid materials could be examined by optical methods. Both entrapped HSA and lipase showed improvements in function with increased ormosil content, indicating that such materials are suitable for encapsulation of lipophilic proteins for optical sensor development.

## Introduction

In the past few years several reports have appeared describing the encapsulation of biomolecules into monoliths derived from tetraethyl orthosilicate (TEOS) or tetramethyl orthosilicate (TMOS).<sup>1–5</sup> Encapsulation protocols generally involved the hydrolysis of the alkoxy-

silane precursors in the absence of added alcohol via sonication. A buffer solution containing the protein of interest was then added to the reaction medium to promote gelation. The addition of buffer brings the pH of the system up to biologically acceptable levels and dilutes the alcohol produced during hydrolysis. In most cases, low-temperature aging over a period of several days or weeks resulted in a durable, optically clear biomaterial which showed good retention of protein activity, as summarized by Avnir et al.<sup>6</sup>

Recently, Reetz and co-workers have published a number of studies which show that adding organically modified silanes (ormosils), such as methyltrimethoxysilane or poly(dimethylsiloxane), to TEOS during the hydrolysis stage can produce a protein-doped organic–inorganic hybrid material which is hydrophobic.<sup>7</sup> These

\* To whom correspondence should be addressed. Telephone: (905) 525-9140 (ext. 27033). Fax: (905) 522-2509. E-mail: brennanj@mcmaster.cis.mcmaster.ca.

<sup>†</sup> McMaster University.

<sup>‡</sup> Brock University.

(1) (a) Narang, U.; Jordan, J. D.; Bright, F. V.; Prasad, P. N. *J. Phys. Chem.* **1994**, *98*, 8101. (b) Lundgren, J. S.; Bright, F. V. *Anal. Chem.* **1996**, *68*, 3377. (c) Jordan, J. D.; Dunbar, R. A.; Bright, F. V. *Anal. Chem.* **1995**, *67*, 2436. (d) Wang, R.; Narang, U.; Prasad, P. N.; Bright, F. V. *Anal. Chem.* **1993**, *65*, 2671. (e) Narang, U.; Prasad, P. N.; Bright, F. V.; Ramanathan, K.; Kumar, N. D.; Malhotra, B. D.; Kamalasanan, M. N.; Chandra, S. *Anal. Chem.* **1994**, *66*, 3139.

(2) (a) Ellerby, L. M.; Nishida, C. R.; Nishida, F.; Yamanaka, S. A.; Dunn, B.; Valentine, J. S.; Zink, J. I. *Science* **1992**, *225*, 1113. (b) Wu, S.; Ellerby, L. M.; Cohan, J. S.; Dunn, B.; El-Sayed, M. A.; Valentine, J. S.; Zink, J. I. *Chem. Mater.* **1993**, *5*, 115. (c) Miller, J. M.; Dunn, B.; Valentine, J. S.; Zink, J. I. *J. Non-Cryst. Solids* **1996**, *220*, 279. (d) Yamanaka, S. A.; Dunn, B.; Valentine, J. S.; Zink, J. I. *J. Am. Chem. Soc.* **1995**, *117*, 9095. (e) Dave, B. C.; Soyuz, H.; Miller, J. M.; Dunn, B.; Valentine, J. S.; Zink, J. I. *Chem. Mater.* **1995**, *7*, 1431. (f) Yamanaka, S. A.; Nishida, F.; Ellerby, L. M.; Nishida, C. R.; Dunn, B.; Valentine, J. S.; Zink, J. I. *Chem. Mater.* **1992**, *4*, 495. (g) Dave, B. C.; Dunn, B.; Valentine, J. S.; Zink, J. I. *Anal. Chem.* **1994**, *66*, 1120A.

(3) (a) Braun S.; Rappoport, S.; Zusman, R.; Avnir, D.; Ottolenghi, M. *Mater. Lett.* **1990**, *10*, 1. (b) Braun, S.; Shtelzer, S.; Rappoport, S.; Avnir, D.; Ottolenghi, M. *J. Non-Cryst. Solids* **1992**, *147*, 739. (c) Avnir, D. *Acc. Chem. Res.* **1995**, *28*, 328.

(4) (a) Edmiston, P. L.; Wambolt, C. L.; Smith, M. K.; Saavedra, S. *J. Colloid Interface Sci.* **1994**, *163*, 395. (b) Wambolt, C. L.; Saavedra, S. *J. Sol-Gel Sci. Technol.* **1996**, *7*, 53.

(5) (a) Zheng, L.; Reid, W. R.; Brennan, J. D. *Anal. Chem.* **1997**, *69*, 3940. (b) Zheng, L.; Brennan, J. D. *Analyst* **1998**, *123*, 1735. (c) Flora, K.; Brennan, J. D. *Anal. Chem.* **1998**, *70*, 4505.

(6) Avnir, D.; Braun, S.; Lev, O.; Ottolenghi, M. *Chem. Mater.* **1994**, *6*, 1605.

(7) (a) Reetz, M.; Zonta, A.; Simpelkamp, J. *Biotechnol. Bioeng.* **1996**, *49*, 527. (b) Reetz, M. T.; Zonta, A.; Simpelkamp, J.; Konen, W. *Chem. Commun.* **1996**, 1397. (c) Reetz, M. T.; Zonta, A.; Simpelkamp, J. *Angew. Chem., Int. Ed. Engl.* **1995**, *34*, 301. (d) Kuncova, G.; Guglielmi, M.; Dubina, P.; Safar, B. *Collect. Czech. Chem. Commun.* **1995**, *60*, 1573.

materials were shown to stabilize lipophilic biomolecules, such as lipase, that did not remain functional in polar matrixes derived from TEOS. However, the hybrid material obtained was opaque, limiting the development of optical sensors which require that the matrix be optically clear, durable, and resistant to fracture during dehydration and rehydration. This was not a concern in the lipase studies since the materials were used as crushed powders for bioreactors.

The use of organically modified alkoxy silane precursors species for developing new sol-gel-derived materials has been increasing rapidly in recent years.<sup>8,9</sup> Numerous articles and reviews have described the use of organotrialkoxysilanes,<sup>10,11</sup> organodisilicates,<sup>12</sup> and polysiloxanes<sup>13</sup> for modification of the properties of sol-gel-derived materials. Several of these studies addressed the issue of optical clarity. However, none of the various protocols described in the literature were amenable to the preparation of optically clear, *protein-doped* organic-inorganic composite materials.

The primary objective of this work is to prepare and characterize optically clear composite materials using protocols which are amenable to protein encapsulation. These protocols include sonication of precursors in the absence of added ethanol, addition of a buffer solution to promote gelation, and low-temperature aging.<sup>1-3</sup> We describe materials prepared from TEOS and one of three different organically modified silane precursors: methyltriethoxysilane (MTES), propyltrimethoxysilane (PTMS), and dimethyldimethoxysilane (DMDMS). These alkylsilanes were chosen to examine the effect of both the length and number of alkyl chains on the properties of the silica matrix (i.e., polarity, hardness, optical clarity, hydration stability), and on the structure and function of entrapped proteins.

Composite materials were characterized using fluorescence and nuclear magnetic resonance (NMR) spectroscopy. Many <sup>29</sup>Si and <sup>13</sup>C NMR studies have appeared recently describing the hydrolysis and condensation reactions of TEOS,<sup>14</sup> MTES,<sup>15</sup> DMDMS,<sup>16</sup> and mixtures of TEOS with MTES.<sup>17</sup> In all previous NMR studies, the solutions were prepared without sonication. The present study extends these previous studies to the case where sonication is used to aid hydrolysis, and examines the internal structure of the final matrix and the presence of unhydrolyzed ethoxy groups using solid-state NMR.

Fluorescence spectroscopy has also been widely applied to the study of sol-gel-derived materials.<sup>18</sup> The present study utilizes 6-propionyl-2-dimethylaminonaphthalene (prodan)<sup>19</sup> and 7-azaindole (7AI),<sup>20</sup> which are both extremely sensitive to local polarity and the presence of protic solvents. 7AI also shows a characteristic emission peak between 410 and 415 nm when the probe adsorbs onto hydroxyl groups present at the surface of the pores within the silicate matrix.<sup>21,22</sup> Thus, 7AI can be used to monitor the presence of silanol groups within the matrix, providing a method to obtain qualitative information regarding the degree of cross-linking. Prodan has the advantage that at high concentrations it will form dimers and/or higher order aggregates which have a unique emission maximum at 420 nm.<sup>23</sup> Thus, prodan is capable of providing information on local solvent concentration and drying rates.

The proteins which were chosen for entrapment into the hybrid materials were human serum albumin (HSA) and lipase. We chose HSA to demonstrate the utility of having optically transparent hybrid materials which allow for straightforward spectroscopic studies of entrapped proteins. HSA is formed from a single polypeptide chain of 585 residues<sup>24</sup> which is divided into 3 major domains, and contains a total of 17 disulfide bonds.<sup>25</sup> Despite the size and complexity of HSA, there is only a single Trp residue within the protein at position 214 in domain II,<sup>24</sup> making it useful for studies involving fluorescence spectroscopy. The fluorescence of the single Trp residue in HSA has previously been used to provide information on the conformation of the protein in solution,<sup>26</sup> and thus should be useful for probing how the structure of entrapped HSA is affected by matrix composition and preparation methods. In addition, the binding of the ligand salicylate quenches Trp fluorescence, and therefore can be used to optically probe protein function, and how this changes with the type and amount of ormosil present.

Lipase was an obvious choice for entrapment since it has previously been demonstrated that this protein shows improved hydrolytic activity when entrapped in organically doped sol-gel media.<sup>7</sup> Lipases can be used for a variety of esterification, interesterification, and hydrolysis reactions, and hence are potentially useful for the development of optical biosensors. We have used a pH indicator method to examine the ability of lipase to catalyze the conversion of glyceryl tributyrates to butyric acid<sup>7d</sup> when the protein was entrapped in materials prepared with varying types and proportions

(8) (a) Livage, J. *Curr. Opin. Solid-State Mater. Sci.* **1997**, *2*, 132. (b) Lev, O.; Tsionsky, L.; Rabinovich, L.; Glezer, V.; Sampath, S.; Pankratov, I.; Gun, J. *Anal. Chem.* **1995**, *67*, 22A.

(9) Schmidt, H. In *Better Ceramics Through Chemistry*; North-Holland: Amsterdam, 1984; Vol. 32, p 327.

(10) (a) Chambers, R. C.; Haruyv, Y.; Fox, M. A. *Chem. Mater.* **1994**, *6*, 1351. (b) Carr, S. W.; Courtney, L.; Sullivan, A. C. *Chem. Mater.* **1997**, *9*, 1751.

(11) (a) Schubert, U.; Husing, N.; Lorenz, A. *Chem. Mater.* **1995**, *7*, 2010. (b) Sugahara, Y.; Inoue, T.; Kuroda K. *J. Mater. Chem.* **1997**, *7*, 53.

(12) Barrie, P.; Carr, S.; Ou, D.; Sullivan, A. C. *Chem. Mater.* **1995**, *7*, 265.

(13) Loy, D.; Jamison, G.; Baugher, B.; Myers, S.; Assink, R.; Shea, K. *Chem. Mater.* **1996**, *8*, 656.

(14) Fyfe, C. A.; Aroca, P. *Chem. Mater.* **1995**, *7*, 1800.

(15) (a) van Bommel, M. J.; Bernards, T. N. M.; Boonstra, A. H. J. *Non-Cryst. Solids* **1991**, *128*, 231. (b) Alam, T. M.; Assink, R. A.; Loy, D. A. *Chem. Mater.* **1996**, *8*, 2366.

(16) Sugahara, Y.; Okada, S.; Kuroda, K.; Kato, C. *J. Non-Cryst. Solids* **1992**, *139*, 25.

(17) Fyfe C. A.; Aroca, P. P. *J. Phys. Chem. B* **1997**, *101*, 9504.

(18) Dunn, B. I.; Zink, J. I. *Chem. Mater.* **1997**, *9*, 2280, and references therein.

(19) Weber G.; Farris, F. J. *Biochemistry* **1979**, *18*, 3075.

(20) (a) Negerie, M.; Gai, F.; Bellefeuille, S. M.; Petrich, J. W. *J. Phys. Chem.* **1991**, *95*, 8663. (b) Chapman, C. F.; Maroncelli, M. *J. Phys. Chem.* **1992**, *96*, 8430. (c) Chen, Y.; Rich, R. L.; Gai, F.; Petrich, J. W. *J. Phys. Chem.* **1993**, *97*, 1770. (d) Rich, R. L.; Chen, Y.; Neven, D.; Negerie, M.; Gai, F.; Petrich, J. W. *J. Phys. Chem.* **1993**, *97*, 1781.

(21) Matsui, K.; Matsuzuka, T.; Fujita, H. *J. Phys. Chem.* **1989**, *93*, 4991.

(22) Flora, K. K.; Dabrowski, M. A.; Musson, S. P.; Brennan, J. D. *Can. J. Chem.*, submitted for publication.

(23) Sun, S.; Heitz, M. P.; Perez, S. A.; Colon, L. A.; Bruckenstein, S.; Bright, F. V. *Appl. Spectrosc.* **1997**, *51*, 1316.

(24) Carter, D. C.; Ho, J. X. *Adv. Protein Chem.* **1994**, *45*, 153.

(25) Brown, J. R. In *Albumin Structure, Function and Uses*; Rosenoer, V. M., Oratz, M., Rothschild, M. A., Eds.; Pergamon: Oxford, 1977; p 27.

(26) Flora, K. K.; Brennan, J. D.; Baker, G. A.; Doody, M. A.; Bright, F. V. *Biophys. J.* **1998**, *75*, 1084.

of organosilane. The results show the utility of entrapping lipase into optically clear organic–inorganic hybrid materials.

### Experimental Section

**Chemicals.** Methyltriethoxysilane (MTES, 99%) and *n*-propyltrimethoxysilane (PTMS, 99%) were obtained from Petrarch Silanes and Silicones (Bristol, PA). Tetraethyl orthosilicate (TEOS, 99.999+) and dimethyldimethoxysilane (DM-DMS, 98%) were obtained from Aldrich Chemicals (Milwaukee, WI). All silanes were used without further purification. Human serum albumin (HSA, 99%, essentially fatty acid free), lipase (from *Candida rugosa*, 60 000 units mg<sup>-1</sup>), glyceryl tributyrate, salicylic acid, 7-azaindole (7AI), and the polymethacrylate and polystyrene fluorimeter cuvettes were obtained from Sigma Chemicals (St. Louis, MO). 6-Propionyl-2-dimethylaminonaphthalene (prodan) was obtained from Molecular Probes (Eugene, OR). All water was purified by reverse osmosis and deionized using a four-stage Elga water purification system. All other chemicals and solvents used were of analytical grade and were used without further purification.

**Procedures.** *Preparation of Precursor Solutions.* Hydrolysis of precursors was done by two methods. In the separate hydrolysis method, the appropriate silane (TEOS, MTES, or PTMS) was hydrolyzed by mixing 4.5 mL of the silane with 1.4 mL of cold deionized water and 0.1 mL of 0.1 N hydrochloric acid and sonicating the mixture in ice water until a clear, single-phase solution was formed. These resulted in molar ratios of H<sub>2</sub>O:Si (*R* values) of 4.1 (TEOS), 3.7 (MTES), and 3.3 (PTMS) during hydrolysis. Pure DMDMS could not be hydrolyzed, as it would not form one clear phase, regardless of how long it was sonicated. Therefore, sol–gel-derived glass materials containing DMDMS were prepared by the cohydrolysis method exclusively. In the cohydrolysis method an appropriate amount of organosilane (MTES, PTMS, or DM-DMS) was first added to TEOS to provide organosilane:TEOS ratios ranging up to 40 vol % for MTES (mole ratio of MTES up to 0.43), up to 10% for DMDMS (mole ratio up to 0.15) and up to 20% for PTMS (mole ratio up to 0.24). A total of 4.5 mL of the silane solution was mixed with 1.4 mL of water and 0.1 mL of 0.1 N HCl and sonicated as described above. These conditions provided *R* values between 4.1 and 3.9 for all samples, with the *R* value decreasing as the proportion of ormosil increased.

In both methods, the sonicated silane solutions were stored for 7 days at –20 °C before use to allow complete hydrolysis of the alkoxy groups to occur. <sup>29</sup>Si NMR spectra of the hydrolyzed solutions were obtained immediately after the solution had become one clear phase, and later to observe the changes that occurred over time under different storage conditions. The pH of the hydrolyzed solutions was assessed using litmus paper, and all solutions were in the pH range of 2.5 ± 0.5. This is in good agreement with the calculated pH of 2.2 which would be expected based on the amount of HCl present.

*Preparation of Monoliths.* Monoliths were prepared from solutions which were kept at 0 °C until the final mixing steps were complete. In the separate hydrolysis method, appropriate volumes of each hydrolyzed silane were combined in a polystyrene cuvette to give a total of 1.0 mL of solution (for blocks) or 300 μL of solution (for slides) with organosilane:TEOS ratios ranging from 0% to 40% (v/v) for MTES (mole ratio of 0 to 0.43) and 0% to 20% (v/v) for PTMS (mole ratio of 0 to 0.24). Alternatively, 1.0 mL or 300 μL of the cohydrolyzed silane solutions was added to the cuvettes. In all cases, an equivalent volume (1.0 mL or 300 μL) of 0 °C phosphate buffer solution (10 mM, 100 mM KCl, pH 7.2) containing either 2 μM of prodan or 30 μM of 7AI were added to the cuvette, and the contents were gently shaken to ensure complete mixing of the two solutions. The addition of the buffer for gelation resulted in the *R* values increasing to between 19 and 21 during gelation for all samples. These values are similar to those typically used for protein entrapment.<sup>1–3</sup> Following the mixing

of the two components, the cuvettes were capped with Parafilm and were allowed to gel at room temperature. Blocks gelled with the cuvette in an upright position, while cuvettes in which slides were made were laid on their side prior to gelation.

For entrapment of proteins the phosphate buffer solution contained either 10 μM HSA or 36 000 units mL<sup>-1</sup> lipase, and again the buffer solutions were added to the hydrolyzed silane solutions in a 1:1 volume ratio as outlined above. The proteins were entrapped only into materials prepared by cohydrolysis of precursors on the basis of fluorescence results (reported below), and to allow for the use of DMDMS. Samples containing HSA or lipase were made as slides (600 μL total volume) only, since these samples were sufficiently thin to allow rapid diffusion of analytes into the matrix.<sup>5a</sup> Following the mixing of the two solutions, the monoliths were allowed to gel as described above.

Following gelation, the blocks or slides were either aged dry without washing or washed with 2 mL of buffer twice to remove entrapped ethanol (24 h for the first wash, 30 min for the second wash) and dry-aged. The buffer used for washing monoliths that contained entrapped fluorescent probes had the appropriate probe present at a concentration similar to that of the entrapped probe to avoid leaching of entrapped probes. All samples containing proteins were washed with fresh buffer to remove the entrapped ethanol, which is known to denature entrapped proteins.<sup>2c</sup> Following the washing steps (or immediately for unwashed samples), the cuvettes were capped with Parafilm and a small hole was punched into the film using a syringe needle. All samples were aged at 4 °C over a period of several months.

*<sup>29</sup>Si Solution Nuclear Magnetic Resonance Spectroscopy.* The 39.76 MHz <sup>29</sup>Si solution NMR spectra of 2–3 mL samples were obtained on a Bruker AC-200 multinuclear Fourier Transform NMR spectrometer using 10-mm glass NMR tubes, and referenced to external TMS. Spectra were obtained using 30° pulses with a 10-s relaxation delay between pulses and a spectral width of 160 ppm. Normally, 360 scans were obtained, but for rapidly evolving samples only 180 scans were obtained. Inverse gated proton decoupling was applied to suppress the nuclear Overhauser effect (NOE). An automated program allowed the desired number of scans to be obtained, followed by a delay (usually 1 h), after which a further spectrum was obtained. This was repeated as many times as desired, typically 10–15 times in an overnight run, to monitor changes in solution composition. The NMR data was manipulated using WIN NMR software, normally with the application of 12 Hz of line broadening.

*Solid-State <sup>29</sup>Si and <sup>13</sup>C NMR.* <sup>29</sup>Si and <sup>13</sup>C cross polarization-magic angle spinning (CP-MAS) spectra of the solids were obtained on a Bruker DPX-300 multinuclear Fourier transform instrument using a Bruker standard bore MAS probe with 4-mm zirconia rotors, at frequencies of 59.62 MHz for <sup>29</sup>Si and 75.50 MHz for <sup>13</sup>C, with proton decoupling during acquisition and referencing to external TMS. Samples were spun at 4 kHz. For <sup>29</sup>Si, an 8-ms contact time was used with a 5-s delay between pulses, and 512 scans were obtained using a spectral window of 18 000 Hz. For <sup>13</sup>C, a 4-ms contact time was used with a 4-s delay between pulses, and 300 scans were obtained with a spectral window of 30 000 Hz.

*Fluorescence Spectroscopy.* Fluorescence spectra were collected, using instrumentation and protocols which are described elsewhere,<sup>5</sup> from samples containing 30 μM of 7AI or 2 μM of prodan which were maintained at a temperature of 20 ± 0.2 °C using a Neslab R110 recirculating water bath. Samples containing 7AI were excited at 290 nm with emission collected from 305 to 560 nm while samples containing prodan were excited at 370 nm with emission collected from 385 to 650 nm. All spectra were collected in 1-nm increments at a rate of 180 nm min<sup>-1</sup>. Appropriate blanks were subtracted from each sample and the spectra were corrected for deviations in emission monochromator throughput and photomultiplier tube response. Emission spectra of fluorophore-doped materials were collected at several times from gelation up to 6 months of aging, while protein-doped samples were tested on day 21.

**Salicylate Titrations of HSA.** All experiments involving salicylate titrations were done with sol-gel-derived slides (dimensions  $\sim 15 \text{ mm} \times 8 \text{ mm} \times 0.2 \text{ mm}$ )<sup>2a</sup> which were aged for 21 days. The samples were placed into polymethacrylate fluorimeter cuvettes containing 2.0 mL of a 10 mM phosphate buffer. The samples were titrated with 100  $\mu\text{M}$  salicylate in 10 mM phosphate buffer at pH 7.2. Fluorescence emission spectra were collected for the protein at various levels of salicylate with excitation at 295 nm and emission collected from 310 to 450 nm to monitor the quenching of Trp by salicylate. The spectra were corrected for blank contributions using a solution containing salicylate but no protein, and a 10-nm window centered about the Trp emission wavelength maximum at  $\sim 335 \text{ nm}$  was integrated to provide intensity values for the protein at each salicylate concentration. Linear regression was performed on each curve to quantitate the relative degree of binding of salicylate to HSA.<sup>27</sup> For comparison, these experiments were repeated for both native and denatured HSA in solution (denatured using 5.0 M guanidine hydrochloride), with appropriate blank subtraction and dilution corrections applied.

**Lipase Activity Assays.** Samples containing lipase were tested as slides (i.e., they were not crushed to powders). The assay involved incubating the lipase-doped slide in a solution prepared by mixing 0.5 mL of glyceryl tributyrate (0.000 17 mol) with 0.5 mL of distilled water. The assay was run for 30 min at 25 °C with continuous stirring. The reaction was then quenched by adding 2.0 mL of a 1:1 (v:v) mixture of ethanol and acetone, and the free fatty acid content was determined by titrating with 0.05 M NaOH to a phenolphthalein endpoint. The average activity values of the entrapped lipase (over five samples) were determined from the volume of NaOH added, and are reported relative to the activity of a solution containing an identical amount of lipase which was assayed in an identical manner.

**Optical Clarity.** UV-vis transmittance spectra of the fully dried sol-gel-derived slides and blocks were collected on an ATI-Unicam UV-4 spectrophotometer at days 21 and 180 after gelation. The instrument was zeroed using empty polymethacrylate cuvettes in the sample and reference paths. All sol-gel-derived samples were run in polymethacrylate cuvettes with an empty cuvette in the reference path. The transmittance at 400 nm was recorded for each sample.

**Hardness.** Hardness of 180-day-old samples was tested qualitatively using the Moh's hardness scale by scratching the surface of the monoliths with various substances. The substances used were talc (1), gypsum (2), calcite (3), copper (3.5), fluorite (4), apatite (5), a glass plate (5.5), orthoclase (6), and quartz (7). The number given in parentheses increases as the hardness of the compound increases. The number assigned to the sol-gel-derived materials is based on the substance for which both the sol-gel product and the substance scratched each other, or neither scratched the other.

**Dehydration/Rehydration Behavior.** A simple qualitative classification of dehydration behavior was obtained by counting the number of cracks which developed in a standard size ( $15 \times 8 \times 0.2 \text{ mm}$ ) slide as drying proceeded. Samples were tested at various times, including day 21 (when protein testing was done) and day 180. Samples which did not crack were classified as excellent, those with 1 or 2 cracks as good, those with 3–5 cracks as moderate, and those with more than 5 cracks as poor. Rehydration stability was determined by rapidly adding 2 mL of buffer solution to the cuvette containing the monolith, and judged by the number of cracks formed during rehydration, using the same scale.

## Results and Discussion

**NMR Studies. Separately Hydrolyzed Materials.** **TEOS.** The <sup>29</sup>Si solution NMR spectrum of the TEOS/water/acid mixture (45/14/1 v/v/v,  $R = 4.1$ ), obtained

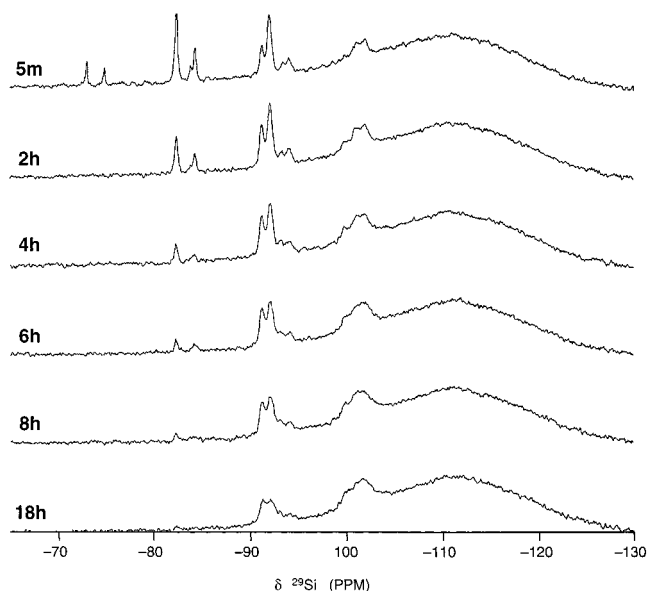


**Figure 1.** The 39.76 MHz <sup>29</sup>Si {<sup>1</sup>H} NMR spectra of TEOS/water/acid (45:14:1 v/v/v) mixture, after sonication for 1 h to form one clear phase. Each spectrum took almost 1 h to acquire. The elapsed time after sonication and before acquisition started is given on each spectrum.

immediately after the 1 h of sonication required to give one phase, shows the presence of a large amount of unreacted TEOS ( $-82.3 \text{ ppm}$ ), along with the hydrolysis products<sup>14,15</sup>  $\text{Si}(\text{OCH}_2\text{H}_5)(\text{OH})_3$  ( $-74.8 \text{ ppm}$ ) and  $\text{Si}(\text{OH})_4$  ( $-72.9 \text{ ppm}$ ), and several condensation products (Figure 1). The condensation products are described according to the  $Q^n$  terminology of Engelhardt,<sup>28</sup> in which  $Q^0$  denotes a silicon with no Si–O–Si linkages,  $Q^1$  denotes a silicon with one Si–O–Si linkage, up to  $Q^4$  which denotes a silicon with four Si–O–Si linkages. The peak at  $-84.3 \text{ ppm}$  arises from  $Q^1$  silicon, those at  $-91.1$ ,  $-91.9$ ,  $-93.2$ , and  $-93.9 \text{ ppm}$  from  $Q^2$  silicon and the  $-99.8$ ,  $-101.1$ , and  $-101.8 \text{ ppm}$  (barely resolved) peaks from  $Q^3$  silicon.<sup>15</sup> Thus, condensation occurs concurrently with hydrolysis. Any  $Q^4$  species which were present might not be detected since their <sup>29</sup>Si signals would occur in the same chemical shift range as the broad high-field peak arising from the glass of the NMR sample tube and NMR probe. Such peaks would also be broad, given that peak widths increase with degree of condensation, consistent with the slower tumbling of the larger condensed species and the resulting shorter spin–spin relaxation times.

Standing at room temperature for various time periods following sonication leads to rapid disappearance of the hydrolysis products (no <sup>29</sup>Si signals after 3 h; Figure 1), and much slower continuation of TEOS condensation to give  $Q^2$  and  $Q^3$  products long after there are no detectable amounts of the hydrolysis products  $\text{Si}(\text{OH})_4$  and  $\text{Si}(\text{OCH}_2\text{H}_5)(\text{OH})_3$  ( $-72.9$  and  $-74.8 \text{ ppm}$ , respectively). Thus sonication generates detectable hydrolysis products, but on standing the sonicated mixture favors condensation over further hydrolysis, i.e., condensation occurs more rapidly than hydrolysis so that hydrolysis products do not build up to a detectable level.

(27) Brown, K. F.; Crooks, M. J. *Biochem. Pharmacol.* **1976**, *25*, 1175.

(28) (a) Engelhardt, G.; Jancke, H.; Hoebbel, D.; Wieker, W. Z. *Chem.* **1974**, *14*, 109. (b) Magi, M.; Lippmaa, E.; Samoson, A.; Engelhardt, G.; Grimmer, A. R. *J. Phys. Chem.* **1984**, *88*, 1518.

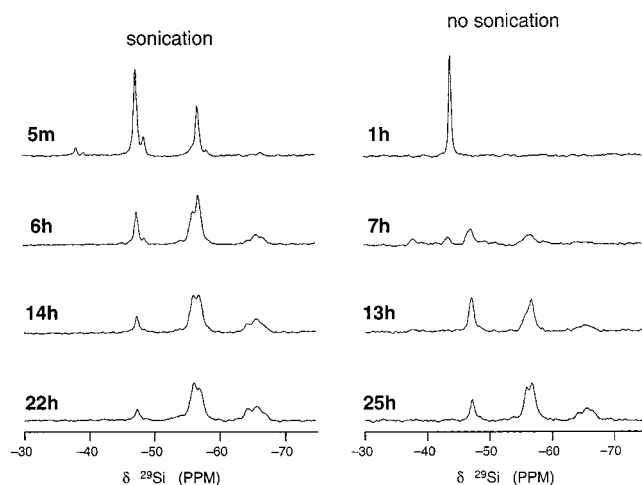


**Figure 2.** The 39.76 MHz  $^{29}\text{Si}$   $\{^1\text{H}\}$  NMR spectra of MTES/water/acid (45:14:1 v/v/v) hydrolysis and condensation. Each spectrum took almost 1 h to acquire: left side, after sonication for 15 min to give one clear phase and, right side, no sonication. The time elapsed after sonication or mixing, and before spectral acquisition, is given on each spectrum.

Fyfe and Aroca<sup>14</sup> reported that the intermediate species  $\text{Si}(\text{OH})_2(\text{OEt})_2$  and  $\text{Si}(\text{OH})_3(\text{OEt})$  never reach molar ratios greater than 10% of the total concentration of all silane species in unsonicated systems, because they react too quickly. In our sonication studies, the  $\text{Si}(\text{OH})_n(\text{OEt})_{4-n}$   $^{29}\text{Si}$  signals never exceed 3% of the total  $^{29}\text{Si}$  intensity.

A solution stored for one week at minus 20 °C gave no  $^{29}\text{Si}$  peaks of unhydrolyzed TEOS (or other initial hydrolysis products). Therefore no further ethanol can be produced from TEOS. There is still the possibility that the condensation products may contain some unhydrolyzed ethoxy groups, but  $^{13}\text{C}$  NMR spectra of these samples show that this fraction is small. Hence, this system should be suitable for use in preparing monoliths which will encapsulate proteins, since it will not continue to generate ethanol after protein entrapment, a situation which could potentially be harmful to the proteins.<sup>29</sup>

**MTES.**  $^{29}\text{Si}$  NMR spectra of MTES/water/acid solutions with  $R = 4$  (Figure 2) show a very different evolution of the same system with an initial 15 min of sonication to form a clear solution (Figure 2, left side), compared to allowing the acid present to promote hydrolysis and condensation without the aid of sonication (Figure 2, right side). The reaction is accelerated and gives different intermediate compositions when the mixture is sonicated, but the final silicon species composition is fairly similar in both cases.

No MTES (−44.1 ppm) is detectable after sonication, and its hydrolysis products  $\text{CH}_3\text{Si}(\text{OH})_3$  (−38.2 ppm)<sup>15</sup> and  $\text{CH}_3\text{Si}(\text{OC}_2\text{H}_5)(\text{OH})_2$  (−39.4 ppm)<sup>15</sup> are detectable only for the first hour after sonication.  $\text{CH}_3\text{Si}(\text{OC}_2\text{H}_5)_2(\text{OH})$  (−40.4 ppm)<sup>15</sup> could not be detected. As with TEOS,  $^{29}\text{Si}$  peaks of condensed species are detectable immediately after sonication, so condensation to form Si–O–Si bonds occurs concurrently with hydrolysis.  $T^n$  terminology is used to describe condensation products of MTES,<sup>30</sup> from  $T^0$  up to  $T^3$  for the maximum possible

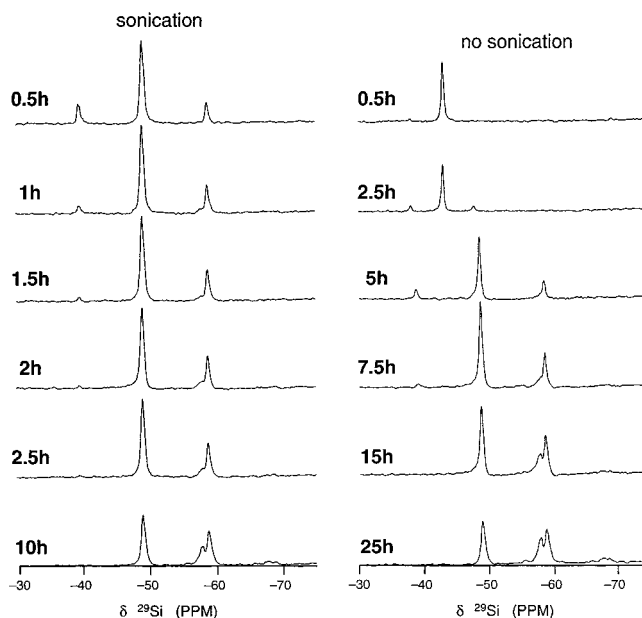


**Figure 3.** The 39.76 MHz  $^{29}\text{Si}$   $\{^1\text{H}\}$  NMR spectra of PTMS/water/acid (45:14:1 v/v/v) hydrolysis and condensation. Each spectrum took 30 min to acquire: left side, after sonication for 5 min to form one clear phase and, right side, no sonication. The time elapsed after sonication or mixing, and before spectral acquisition, is given on each spectrum.

number of Si–O–Si linkages, by analogy with the  $Q^n$  terminology for silicates described above. With sonication there is a gradual diminution of  $T^0$  (−38.2, −39.3, and −43.5 ppm) and  $T^1$  species (−47.4 and −48.7 ppm) and buildup of  $T^2$  (−56.9 and −58.2 ppm) and  $T^3$  (−64.3, −65.7, and −66.7 ppm) (Figure 2). The  $T^1$ ,  $T^2$ , and  $T^3$  site chemical shifts agree well with those reported previously.<sup>15</sup> In this case, unlike TEOS, the entire range of condensation products could be observed with no interference from the broad signal from glass.

Without sonication, MTES diminishes gradually and is still detectable 6 h after mixing (Figure 2). At this time, a small amount of MTES remains, as well as  $T^0$  hydrolysis products at −38.2 ppm and −44.1 ppm,  $T^1$  species at −47.2 ppm, and  $T^2$  species at −56.8 ppm. After 10 h, hydrolysis products are no longer detectable, and the concentration of condensation products ( $T^1$  to  $T^3$ ) increases. Note that the highly condensed  $T^3$  sites build up more slowly without sonication.

**PTMS.** Solutions of *n*-propyltrimethoxysilane (PTMS) required 5 min of sonication to form one clear phase, or without sonication would form a miscible solution in under 4 h at room temperature.  $^{29}\text{Si}$  NMR spectra (Figure 3) show that no PTMS remained after sonication, while hydrolysis products are observable only for the first 2.5 h after sonication. Within 30 min after sonication,  $T^1$  and  $T^2$  groups are observed at −48.9 and −58.7 ppm, respectively. Two hours after sonication,  $T^3$  groups (−68.7 ppm) are just beginning to appear in the spectra. Ten hours after sonication condensation continues slowly with the  $T^3$  group gradually becoming larger with respect to the  $T^1$  and  $T^2$  groups which are still dominant.

PTMS samples which were not sonicated gave a  $^{29}\text{Si}$  peak for hydrolysis products at −38.0 ppm within the

(29) Zheng, L.; Flora, K.; Brennan, J. D. *Chem. Mater.* **1998**, *10*, 3974.

(30) Pursch, M.; Jager, A.; Schneller, T.; Brindle, R.; Albert, K.; Lindner, E. *Chem. Mater.* **1996**, *8*, 1245.

first half hour after the components were mixed. This peak remained until  $\sim 9$  h after mixing. Figure 3 shows that the PTMS  $^{29}\text{Si}$  signal was present in the spectra at  $-43.0$  ppm until almost 5 h after mixing. A small amount of T<sup>1</sup> groups began to appear between 1 and 1.5 h after mixing. Within 3 h after mixing, T<sup>2</sup> species were present, while T<sup>3</sup> species appeared in the spectrum 7.5 h after the three components were mixed. Ten hours after mixing, neither PTMS nor hydrolysis products remained. After this time, condensation slowly continued. On the basis of the  $^{29}\text{Si}$  NMR spectra of the separately hydrolyzed silane species, three main conclusions can be drawn: (i) Sonication of precursors increases the rate of both hydrolysis and condensation reactions regardless of the silane used. This is likely the result of cavitation and local heating during sonication which promote the hydrolysis reaction, coupled with improved miscibility of components during sonication. (ii) The rate of hydrolysis depends on the R group, in the order PTMS > MTES > TEOS. This effect is likely based on inductive effects of the R group which stabilize the transition state during hydrolysis, but may also be partially determined by the size of the leaving group (ethoxy vs methoxy) and slight differences in the iso-electric points of the species. (iii) No unhydrolyzed monomer or unhydrolyzed low order condensation products remain after 1 week.

We cannot exclude the possibility that some of the higher order condensation products may contain unhydrolyzed OEt groups. However, on the basis of the lack of low-order species with OEt groups, the amount of ethanol that could be produced after gelation is likely to be minimal.

**Cohydrolyzed Materials. MTES/TEOS and PTMS/TEOS.** The solution  $^{29}\text{Si}$  NMR spectra of cohydrolyzed systems are a good superposition of the spectra of the separately hydrolyzed materials, with no clear evidence of additional signals due to composite species containing both TEOS and the alkylated silicon component. This is not surprising because of the broadness of the condensed species  $^{29}\text{Si}$  signals and the small  $^{29}\text{Si}$  chemical shift difference ( $\ll 1$  ppm) expected for carbon-for-oxygen substitution separated by 3 bonds from the  $^{29}\text{Si}$  being observed.<sup>31</sup> These results do not exclude the existence of composite condensation products, they merely indicate that  $^{29}\text{Si}$  NMR is not able to resolve the peaks associated with these species.

**DMDMS/TEOS.** DMDMS alone would not form one clear phase, regardless of sonication time, in agreement with the results of Sakka and co-workers who assumed this to be due to the formation of insoluble cyclic poly(dimethylsiloxane) species.<sup>32</sup> DMDMS systems were therefore studied primarily through cohydrolysis in the presence of TEOS. These mixtures were first sonicated and formed clear solutions with up to 25% DMDMS present. As the DMDMS concentration increased, the solution required longer sonication times to form one clear phase. The  $^{29}\text{Si}$  NMR spectra of these samples showed that this increased length of time resulted in

the majority of the TEOS hydrolysis products condensing.  $^{29}\text{Si}$  NMR spectra of mixed DMDMS and TEOS solutions obtained after 20 min of sonication showed neither DMDMS ( $-1.8$  ppm) nor any DMDMS hydrolysis products, which usually occur at  $-3.3$  and  $-4.2$  ppm.<sup>16</sup> The D<sup>1</sup> species were present at approximately  $-12.6$  ppm (lit.<sup>16</sup>  $-12.4$  ppm), while D<sup>2</sup> species arise as a broad peak observed between  $-17.1$  ppm to  $-21.1$  ppm (lit.<sup>16</sup>  $-20.7$  ppm). On further standing, the D<sup>1</sup> signal disappears over a period of 12 h.

**Solid-State NMR.**  $^{29}\text{Si}$  CP-MAS spectra of fully aged TEOS-derived monoliths show the presence of Q<sup>2</sup>, Q<sup>3</sup>, and Q<sup>4</sup> silicon sites, most of the silicon being in the Q<sup>3</sup> and Q<sup>4</sup> sites. The chemical shifts were similar to literature values, and the Q<sup>2</sup> and Q<sup>3</sup> chemical shifts were similar to those observed in solution. Similar correspondences with solution chemical shifts, and with literature values where available, were found for the MTES and PTMS systems. Cohydrolyzed samples show the presence of Q<sup>2</sup>, Q<sup>3</sup>, and Q<sup>4</sup> sites as well as T<sup>2</sup> and T<sup>3</sup> sites (or D<sup>2</sup> sites in the case of DMDMS/TEOS), with  $^{29}\text{Si}$  chemical shifts that correspond well in most cases to our solution values and to literature values. Thus sonication gives materials similar in structure to materials obtained by other methods.

However, because cross polarization involves transfer of magnetization from  $^1\text{H}$  to the X-nucleus ( $^{29}\text{Si}$  or  $^{13}\text{C}$ ) via a dipole-dipole mechanism which is critically dependent on the distance between the proton and the X nucleus,<sup>33</sup> relative CP-MAS NMR peak areas need not correspond to relative amounts of species present. We consistently find discrepancies in relative  $^{29}\text{Si}$  peak areas in two situations: (i) In TEOS-derived materials, Q<sup>4</sup> sites (with no nearby protons) cross polarize less efficiently than Q<sup>2</sup> and Q<sup>3</sup> sites (with OH protons) and give relative  $^{29}\text{Si}$  CP-MAS signals which are much smaller, with respect to the Q<sup>2</sup> and Q<sup>3</sup> sites, than in spectra obtained using high-power  $^1\text{H}$  decoupling alone, without cross polarization. (ii) In materials prepared from mixtures of precursors, the Q sites derived from TEOS always have smaller relative intensities than the T or D sites derived from the organosilanes, compared to those expected from the relative proportions of the precursors. The protons on the alkylsilicon chains contribute to cross polarization to  $^{29}\text{Si}$  and enhance the organosilane signals.

$^{13}\text{C}$  CP/MAS spectra provide information on completeness of hydrolysis by the presence or absence of alkoxy group  $\alpha$ -carbon signals in the 50–60 ppm range. Spectra of samples which were dried either at room temperature or in the refrigerator for a long period of time (180 days) give no detectable alkoxy carbon signal, indicating negligible residual alkoxy groups. This is true for samples prepared from cohydrolyzed as well as from separately hydrolyzed silanes. However rapid drying (24 h under vacuum in a desiccator) does not allow sufficient time for complete hydrolysis. Alkoxy group  $\alpha$ -carbon signals at 58 ppm (sharp) and 60 ppm (broad) in such samples were still present after a week of standing at

(31) Harris, R. K.; Kennedy, J. D.; McFarlane, W. In *NMR and the Periodic Table*; Harris R. K., Mann, B. E., Eds.; Academic Press: London, 1978; p 324.

(32) Sakka, S.; Tanaka, Y.; Kokubo, T. *J. Non-Cryst. Solids* **1986**, *82*, 24.

(33) (a) Fyfe, C. A. *Solid-State NMR for Chemists*; CFC Press: Guelph, Canada, 1983. (b) Clayden, N. J. Special Applications. In *NMR Basic Principles and Progress*; Diehl, P., Fluck, E., Gunther, H., Kosfeld, R., Seelig, J., Eds.; Springer-Verlag: London, 1993; Vol. 29, p 91.

room temperature open to the atmosphere, which would remove any residual alcohol. The signals must therefore arise from alkoxy groups bonded to silicon. Thus rapid drying should be avoided in preparing encapsulated protein systems, since the protein might later be exposed to alcohol from hydrolysis of the residual alkoxy groups.

**Gelation Times.** The major factors affecting the rate of gelation of the hydrolyzed silane when mixed with the buffer solution were the ratio and type of organosilane present in the silane solution, the concentration of buffer used, and the temperature at which monoliths were formed. Gelation times for cohydrolyzed and separately hydrolyzed systems were identical, within experimental error. The gelation time increases as the amount of organosilane added is increased or as buffer concentration is decreased, consistent with previous reports.<sup>8a</sup> The gelation time also increases from MTES to PTMS to DMDMS, suggesting that steric effects partially control the gelation kinetics.<sup>8a</sup> Interestingly, the gelation time decreases for samples containing greater than 7.5% DMDMS, suggesting a phase separation which causes gelation of the two phases to occur independently of each other.

Solution temperature was also a major factor determining gelation time. If the components were both at room temperature ( $22 \pm 1$  °C) and were allowed to gel at room temperature, gelation occurred over fairly short time periods (<5 min for TEOS using 10 mM phosphate buffer). In cases where both solutions were at 0 °C before mixing, and were allowed to gel at room temperature, the gelation times increased by 3-fold, ranging from 10 to 15 min. Gelation at 0 °C was slower still (~30 min). However, slides produced by this method were uneven. Therefore, the method adopted for the formation of monoliths was to keep all solutions on ice until mixing was complete, and then allow gelation to proceed outside of the ice bath. Using these conditions, gelation times ranging from 5 min to greater than 60 min were accessible, and could be controlled by adjustment of the buffer concentration. Such gelation times are useful for protein encapsulation since longer gelation times can cause protein denaturation due to excessive exposure to EtOH, while shorter gelation times may not allow sufficient time for dip-casting (if thin films are desired) or other manipulations.

#### Physical Characteristics of Hybrid Materials.

**Hardness.** Hardness values for the various cohydrolyzed and separately hydrolyzed organosilane samples are given in Tables 1 and 2, respectively. Samples prepared from TEOS alone have a hardness of 4, while ordinary glass has a hardness of 5.5. However, glass has been heat-treated and thus is densified. The hardness of samples made from cohydrolyzed silanes was equivalent to samples made from separately hydrolyzed silanes. In both cases, the hardness of the sample decreased with increased organosilane content, and also decreased as the number or length of the alkyl chains increased. In general, the hardness decreased smoothly as the organosilane content increased, with no significant breaks in the trend which would indicate phase separation. However, the hardness of samples containing DMDMS or PTMS was substantially lower than for those containing equivalent amounts of MTES, suggesting that

**Table 1. Physical Properties of Monoliths Which Were Prepared by Cohydrolysis of TEOS and Organosilanes Which Were Washed or Unwashed after Gelation and Dry-Aged for 180 Days**

sample	optical transmittance (%) <sup>a</sup>	dehydration stability	rehydration stability	hardness (Moh's scale)
TEOS	67/78 <sup>b</sup>	excellent	excellent	4
5% MTES	66/78	excellent	good	3.5
10% MTES	69/80	good	poor	3
15% MTES	64/81	good	poor	3
20% MTES	66/83	good	poor	3
25% MTES	65/81	good	poor	2.5
30% MTES	60/72	moderate	poor	2.5
35% MTES	51/60	moderate	poor	2.5
40% MTES	28/33	poor	—	2
2.5% DMDMS	62/71	good	moderate	3.5
5% DMDMS	51/66	poor	—	3
7.5% DMDMS	24/33	poor	—	3
10% DMDMS	0/0	poor	—	2
5% PTMS	49/60	moderate	poor	2.5
10% PTMS	29/31	poor	—	1.5
15% PTMS	0/0	poor	—	<1
20% PTMS	0/0	poor	—	<1

<sup>a</sup> Transmittance at 400 nm for samples which were 5 mm thick.

<sup>b</sup> First number is for washed samples, second number is for unwashed samples.

**Table 2. Physical Properties of Monoliths Which Were Prepared by Separate Hydrolysis of TEOS and Organosilanes Which Were Washed or Unwashed after Gelation and Dry-Aged for 180 Days**

sample	optical transmittance <sup>a</sup>	dehydration stability	rehydration stability	hardness (Moh's scale)
TEOS	70/80 <sup>b</sup>	excellent	good	4
5% MTES	69/81	excellent	good	3.5
10% MTES	72/80	excellent	moderate	3
15% MTES	71/80	excellent	poor	2.5
20% MTES	67/79	excellent	poor	2.5
25% MTES	65/78	excellent	poor	2.5
30% MTES	58/70	moderate	poor	2.5
35% MTES	50/63	poor	—	2.5
40% MTES	21/29	poor	—	2.5
5% PTMS	52/63	good	moderate	2
10% PTMS	27/36	moderate	poor	2
15% PTMS	0/0	poor	—	<1
20% PTMS	0/0	poor	—	<1

<sup>a</sup> Transmittance at 400 nm for samples which were 5 mm thick.

<sup>b</sup> First number is for washed samples, second number is for unwashed samples.

presence of the additional organic components (more R groups per Si, or longer chains) weakens the Si—O—Si bond network owing to the bulk of the R groups.

**Optical Clarity of the Resultant Glass.** The method used to prepare the monoliths has significant effects on the clarity of the resultant glass, as shown in Tables 1 and 2. The clarity of all samples was improved when the solutions used to make the monoliths were kept at 0 °C until added to the cuvettes. In addition, samples prepared with TEOS which had remained in the freezer longer and therefore had already begun condensing were more transparent than those made from TEOS which was more recently hydrolyzed (1 h of hydrolysis). Furthermore, cohydrolyzed samples were always more transparent than samples which were prepared from separately hydrolyzed silanes. Finally, the clarity of the monoliths was dependent on whether the samples were washed with buffer solution after gelation. Washing the samples had the effect of decreasing the clarity of the glass. This may be the result of the buffer solution

forcing out ethanol which acted as a cosolvent, causing an increase in phase separation behavior in the early stages of monolith formation.

The other major factors affecting the clarity of the glass are the type and content of organosilane and, for gels made from separately hydrolyzed silanes, the order of addition of components. The optimal mixing method was to first add the required volume of buffer into the cuvette, followed by the MTES (or other ormosil), and then TEOS. In all cases, the optical transparency of the organosilicate samples decreased with an increase in organosilane content. The type of organosilane also affected the clarity of the glass. For example, samples containing up to 25% MTES remained quite transparent, while samples containing 10% DMDMS or 15% PTMS were generally opaque. In all cases, the decrease in transparency was fairly abrupt, likely signifying that a separation of phases had occurred. The maximum ratio before decreased clarity occurred correlated roughly to the expected miscibility of the organosilane with TEOS (25% for MTES, 10% for PTMS, and 7.5% for DMDMS), supporting the above suggestion.

*Dehydration/Rehydration Stability.* Tables 1 and 2 show the degree of cracking during dehydration and rehydration for cohydrolyzed and separately hydrolyzed samples containing varying types and ratios of organosilane. Increases in either the number of methyl groups or in the chain length of the organic group resulted in significantly poorer dehydration stability, likely due to a combination of less cross-linking (for DMDMS) and phase separation (for both organosilanes). For MTES, the extent of cracking increased with increased organosilane content. However, there was an obvious discontinuity at a MTES ratio of 20%, consistent with phase separation, above which severe cracking occurred.

The monoliths follow the trend of increased cracking with increased organosilane content, whether made from cohydrolyzed or separately hydrolyzed silanes. However, monoliths made from separately hydrolyzed silanes show less cracking during dehydration than monoliths made from cohydrolyzed silanes. Although the cause of this difference in behavior is not yet fully understood, this is a useful empirical finding with regard to the development of durable, fracture resistant materials. Much of the cracking that occurs during dehydration is likely due to uneven drying of the samples, and the resulting differences in hydrostatic pressure. Hence, improvements in cracking behavior can likely be realized by optimization of drying conditions.

The rehydration behavior of the monoliths generally follows the trend observed for dehydration, despite the changes in water content being very abrupt compared to dehydration, which occurred over a period of several weeks. Rehydration was done first at day 21 when the monoliths still had some water trapped within the pores. This day was chosen since it corresponded to the day that protein-doped samples were rehydrated for testing. Samples were also tested at day 180 when the monoliths were fully dry. Rehydration of partially dried monoliths did not cause further cracking of monoliths which had not already cracked during dehydration. Monoliths could be prepared with up to 20% MTES, 5% DMDMS, or 10% PTMS with no cracking during dehydration or

rehydration (at day 21), regardless of whether the monoliths were prepared with separately hydrolyzed or cohydrolyzed silanes. Above these levels, most monoliths showed extensive cracking during dehydration by day 21, and further cracking upon rehydration.

The rehydration behavior of the fully dried materials at day 180 was far worse than that of the partially dried materials at day 21. The rapid addition of water to fully dried materials caused almost all compositions to shatter due to capillary stress.<sup>34</sup> Compositions containing up to 5% MTES (cohydrolyzed) or 10% MTES (separately hydrolyzed) showed reasonably good rehydration behavior, although only pure TEOS-derived materials were able to fully withstand rehydration without cracking.

Since allowing the materials to dry fully usually results in cracking on rehydration, monoliths should be only partially dried and then stored at 100% humidity, or perhaps in buffer solution, to avoid further drying. This storage method will be required in any event when proteins are entrapped, since proteins normally cannot withstand complete dehydration without a significant loss of activity.

**Internal Environment.** *7-Azaindole Fluorescence.* Representative spectra of 7AI in unwashed and washed cohydrolyzed monoliths that had been dried for 180 days are shown in Figure 4, parts a and b, respectively. Wavelength emission maxima and fwhm values for all samples are given in the Supporting Information. Significant differences are observed based on (i) the organosilane content, (ii) whether samples were washed or unwashed, and (iii) whether samples were prepared from cohydrolyzed or separately hydrolyzed silanes.

Immediately after gelation, the emission maxima were in the range between 360 and 380 nm for all samples, and did not depend on whether samples were washed or unwashed. However, the spread in the values was far greater for cohydrolyzed samples (20 nm) as compared to separately hydrolyzed samples (4 nm). In samples containing MTES or DMDMS, the wavelength of maximum emission was not dependent on the concentration of organically modified silane, suggesting that the internal solvent composition dominated the emission behavior. However, for PTMS samples, the emission wavelength maximum blue-shifted as the proportion of PTMS increased, reflecting the lower dipolarity of the local environment in the presence of increased levels of PTMS.

As the monoliths dried, the wavelength of maximum intensity tended to red-shift for samples containing a low proportion of organically modified silane (20% MTES or less) and to both broaden and blue-shift for samples containing a higher proportion (30% MTES or above). The red-shift at low organosilane contents is consistent with the probe adsorbing onto the silanol groups present on the internal surfaces of such monoliths.<sup>21</sup> This conclusion is supported by the fact that washing of samples results in smaller red-shifts in the emission wavelength, corresponding to a lower silanol content. This is in agreement with a recent report from our group which indicates that the emission wavelength of 7AI and the proportion of silanol groups in aged

(34) Zarzycki, J.; Prassas, M.; Phalippou, J. *J. Mater. Sci.* **1982**, *17*, 3371.



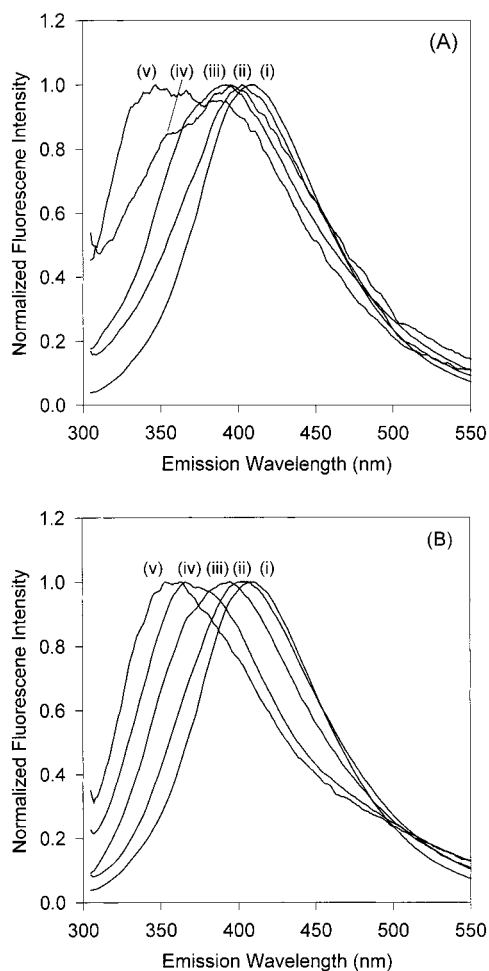


**Figure 4.** (A) Fluorescence spectra of 7-azaindole in un-washed, cohydrolyzed monoliths containing varying amounts of MTES in TEOS after 180 days of aging: (i) 0% MTES, (ii) 10% MTES, (iii) 20% MTES, (iv) 30% MTES, and (v) 40% MTES. (B) Fluorescence spectra of 7-azaindole in washed, cohydrolyzed monoliths containing varying amounts of MTES in TEOS after 180 days of aging: (i) 0% MTES, (ii) 10% MTES, (iii) 20% MTES, (iv) 30% MTES, and (v) 40% MTES.

TEOS monoliths decreases with increased amounts of water present during aging.<sup>22</sup> The spectral broadening and overall blue-shift observed from samples with higher organosilane concentrations is consistent with probe preferentially partitioning to the organic regions rather than adsorbing to the hydroxylated surface. However, there is clearly a distribution of probe between at least two environments of differing dipolarity. The spectral broadening may be an indicator of microscopic phase separation. This interpretation is discussed further below.

7AI in cohydrolyzed and separately hydrolyzed samples containing MTES did not show substantially different spectral properties after aging was completed. In general, both types of samples showed a fairly consistent trend of more blue-shifted emission maxima with increased MTES content, and also show similar emission maxima for samples containing low amounts of DMDMS as compared to similar samples containing double the amount of MTES. Substantially different spectral characteristics were observed for 7AI only when samples contained PTMS. This is to be expected given the lower miscibility of PTMS with TEOS, and thus the higher propensity for phase separation when separate hydroly-

sis of precursors is done. Such characteristics are consistent with the physical properties described above for samples containing PTMS.

The most dramatic differences in 7AI emission characteristics were observed between washed and un-washed samples of similar alkylsilane content which were made by either the cohydrolysis or separate hydrolysis method. The data clearly show that washing of samples causes major changes in the internal environment of the samples, even after drying for 180 days. These changes were most pronounced for cohydrolyzed samples. Spectra collected from unwashed samples showed an increasingly broader spectral contour as the level of MTES (or PTMS, spectra not shown) increased. As the level of MTES increases, the spectra change in a manner which is consistent with the growth of a new peak in the region of 340–350 nm, with a gradual loss of intensity in the main peak in the region of 370–380 nm. The spectral shapes are consistent with partitioning of the probe between a hydrophobic, organosilane-rich region, and a second region of higher dipolarity, likely composed mainly of silica. The spectral breadth may also reflect the presence of peaks which correspond to the adsorbed and soluble forms of the probe.

In cases where the samples were washed for the first 10 days before drying, the spectra are much narrower and show a more gradual progression to shorter emission wavelength maxima. Several reasons can be put forward to explain this trend. First, the presence of excess water from washing over the first 10 days removes any excess ethanol produced as a byproduct of hydrolysis, thus reesterification and the resulting changes in internal environment are avoided. Second, the presence of excess water during the initial stages of aging reduces the proportion of silanol groups, resulting in less potential for adsorption of the 7AI probe, and hence a narrower distribution of states for the probe. Third, the presence of 7AI during the early stages of aging may have provided more favorable conditions for partitioning of the probe from the aqueous solvent into the hydrophobic regions of the monolith (since little or no ethanol is present), resulting in a narrower distribution of probe environments.

The spectra of washed or unwashed separately hydrolyzed samples (not shown) show similar trends to those obtained from similarly aged cohydrolyzed samples. However, there were some notable differences. For example, the spectral width of separately hydrolyzed samples was, in general, broader than that obtained for cohydrolyzed samples. Spectra obtained from unwashed samples containing MTES were particularly broad, with full-width-at-half-maximum (fwhm) values as great as 150 nm (as compared to ~100 nm for similar cohydrolyzed samples). The spectra were quite flat across the top, over a wavelength range of ~60 nm, indicating a large distribution of environments with differing polarity.

In comparing the internal environment from separately hydrolyzed and cohydrolyzed samples, with or without washing, as determined from 7AI emission spectra, three main conclusions can be drawn. First, samples prepared from cohydrolyzed samples provide a narrower distribution of environments, allowing better control over the internal environment. Second, both

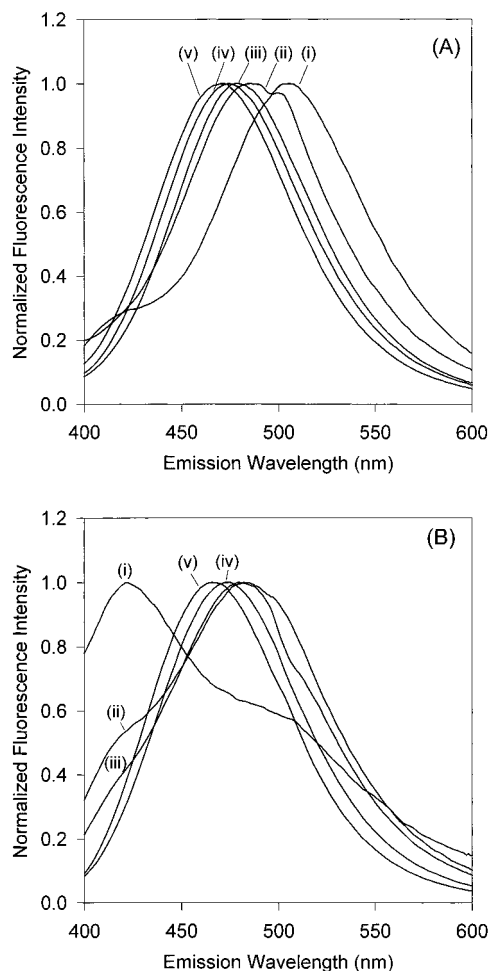


**Figure 5.** (A) Fluorescence spectra of prodan in unwashed, cohydrolyzed monoliths containing varying amounts of MTES in TEOS after 180 days of aging: (i) 0% MTES, (ii) 10% MTES, (iii) 20% MTES, (iv) 30% MTES, and (v) 40% MTES. (B) Fluorescence spectra of prodan in washed, cohydrolyzed monoliths containing varying amounts of MTES in TEOS after 180 days of aging: (i) 0% MTES, (ii) 10% MTES, (iii) 20% MTES, (iv) 30% MTES, and (v) 40% MTES.

separately hydrolyzed and cohydrolyzed samples show controllable decreases in internal polarity with increases in organosilane content. Third, it is evident that washing of monoliths after gelation results in better control of the final internal environment, which is a useful finding when such materials are to be used for entrapment of biomolecules. Washing to remove ethanol is also likely to be beneficial for protein function, since ethanol is known to denature proteins.<sup>2c</sup>

**Prodan Fluorescence.** Representative spectra of prodan in unwashed and washed cohydrolyzed monoliths that had been dried for 180 days are shown in Figure 5, parts a and b, respectively. As with 7AI, significant differences are again observed on the basis of the organosilane content, sample washing, and hydrolysis method. Initially, the emission maximum of prodan in freshly prepared monoliths ranged from 512 nm (TEOS) to 505 nm (40% MTES). The trend of shorter emission wavelength maxima for increasing organosilane content is also observed for samples containing DMDMS or PTMS. This result indicates that the initial environment is affected by the presence of the organosilane, and that the internal environment is determined by both the

ethanol content and the number of organic groups present. Upon aging for 180 days, both separately hydrolyzed and cohydrolyzed samples show a general trend of shorter emission wavelength with increased organosilane content, with the emission maximum gradually shifting from 506 nm in TEOS-derived monoliths to 471 nm in monoliths containing 40% MTES.

Emission spectra of prodan obtained from separately hydrolyzed samples were usually broader than the corresponding spectra for the cohydrolyzed samples in agreement with the results obtained for 7AI spectra. This trend likely reflects the partitioning of prodan between regions which are depleted or enriched in MTES. The broadening of the prodan emission spectra confirms that the internal environment of separately hydrolyzed materials has a wider distribution of local polarities, suggesting that segregation of organosilane components (i.e., phase separation) may be occurring.

The most obvious difference in prodan emission spectra was based on whether samples were washed during the initial stages of aging. In all cases, samples with low organosilane contents show two distinct peaks in the emission spectrum, one near 500 nm, and the other near 420 nm, which change in proportion as the samples age. However, in washed samples the peak at 420 nm is dominant in TEOS-derived samples, and is evident in samples containing up to 20% MTES. For unwashed samples, the peak at 420 nm is much less pronounced, and is only evident in samples containing up to 10% MTES. The 420-nm peak has recently been reported to be due to prodan forming microcrystals, higher order aggregates and/or dimers in water when the concentration of probe exceeds about  $1 \mu\text{M}$ .<sup>23</sup> Hence, it is expected that increases in the content of MTES should cause the peak at 420 nm to decrease in intensity, due to the increased solubility of prodan in the organic phase. The larger dimer peaks in dried monoliths that were washed suggests that higher levels of water during the initial stages of aging promotes aggregation of the probe, likely due to the removal of ethanol from the internal regions of the monoliths. These aggregates, once formed, are quite stable, since the dimer/aggregate peak does not completely disappear, even after drying for 180 days.

An interesting aspect of the peaks corresponding to monomer and aggregated forms of prodan is that their ratio changes over time, as shown in Figure 6. Thus, the ratio of monomer and dimer peaks provides a sensitive method for probing the amount of water remaining inside the monoliths of high polarity. The intensity ratio of the aggregate and monomer peaks increases rapidly over the first 30 days for most samples and then remains relatively constant or decreases slightly as drying proceeds. The initial increases are largest for samples containing low organosilane content, as described above. The initial increases in the aggregate-to-monomer ratio, and the shift to lower wavelengths for the monomer peak during aging, are consistent with ethanol and water being removed over the first 30 days, and are in good agreement with the changes in monolith mass over this period of time. The smaller changes in the ratio observed after day 30 are consistent with a slow repartitioning of the probe between dimer and monomer forms, free and adsorbed

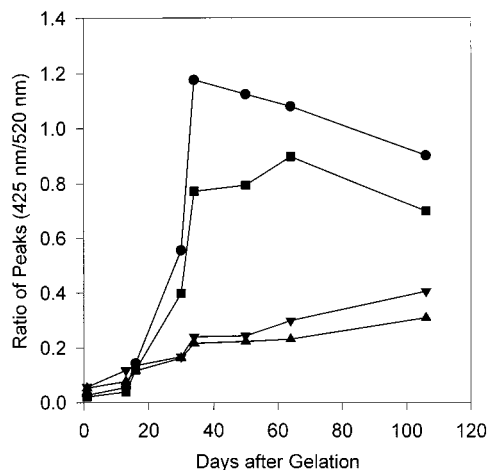


**Figure 6.** Ratio of the aggregate and monomer peaks of prodan in MTES:TEOS monoliths as a function of drying time: (●) 0% MTES, (■) 10% MTES, (▼) 20% MTES, and (▲) 40% MTES.

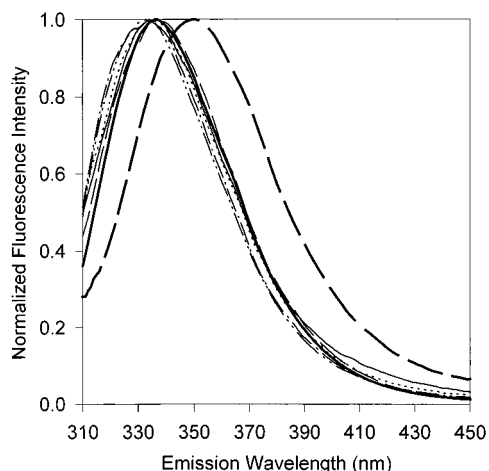


**Figure 7.** Fluorescence emission spectra of HSA entrapped into sol-gel-derived hybrid materials prepared by the cohydrolysis method: (—) HSA in solution, (---) denatured HSA, (---) TEOS, (- - -) 10% MTES, (···) 20% MTES, (-·-·) 5% DMDMS, and (-·-·) 10% PTMS.

states, and possibly between MTES-enriched and -depleted areas when this component is present.

**Characteristics of Entrapped Proteins.** *HSA.* On the basis of the results obtained from 7AI fluorescence studies, and on the need to use cohydrolyzed samples to investigate the effects of DMDMS, all samples were formed from cohydrolyzed precursor solutions and were washed after gelation. Only those samples that had shown good physical characteristics on day 21 (i.e., up to 20% MTES, 10% PTMS, 5% DMDMS) were further investigated. Figure 7 shows the background-corrected and normalized fluorescence emission spectra obtained from HSA that was entrapped in these samples. The emission spectra of both native HSA (thick solid line) and guanidine denatured HSA (thick broken line) in solution are shown for comparison. The emission spectra of the entrapped HSA samples are all similar to the spectrum of native HSA in solution, with only slight blue shifts and small increases in the fwhm values as ormosil content increased. Specific emission maximum values were as follows: native HSA = 337 nm, denatured HSA = 345 nm, TEOS = 337 nm, 10% MTES = 337 nm, 20% MTES = 334 nm, 10% PTMS = 334 nm,

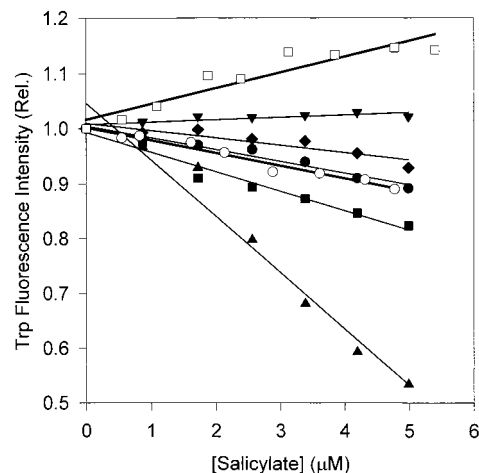


**Figure 8.** Changes in HSA fluorescence intensity resulting from quenching by salicylate upon binding: (○) HSA in solution (slope =  $-0.023$ ), (□) denatured HSA (slope =  $0.028$ ), (●) TEOS (slope =  $-0.021$ ), (■) 10% MTES (slope =  $-0.036$ ), (▲) 20% MTES (slope =  $-0.103$ ), (◆) 5% DMDMS (slope =  $-0.013$ ), and (▼) 10% PTMS (slope =  $0.004$ ).

5% DMDMS = 333 nm. These results provide two important pieces of information: (i) the sol-gel-derived hybrid materials are suitable for spectroscopic studies of entrapped proteins, even when excitation is done in the ultraviolet region of the spectrum, where light scattering is the highest, and (ii) based on the similarity in emission spectra, HSA appears to be entrapped with retention of its native conformation, regardless of the ormosil type or content.

Salicylate binding to the entrapped protein was done to probe the protein function, and these results were compared to those obtained for native and denatured HSA in solution. Since the samples were optically clear, binding could be monitored spectroscopically by quantitating the change of intensity for the Trp residue resulting from binding of salicylate, as shown in Figure 8. The slopes of the binding curves, given in the caption to Figure 8, showed that most samples retained at least partial function as compared to HSA in solution, indicating that the entrapment method did not completely alter the functional form of the protein. HSA entrapped in TEOS-derived materials showed similar sensitivity to salicylate binding as compared to the protein in solution, suggesting that TEOS had no major affect on HSA behavior. Entrapment of HSA in the presence of DMDMS, and particularly PTMS, caused a reduction in protein function, likely indicating that HSA becomes partially denatured as a result of the presence of longer alkyl chains. It is well-known that HSA is denatured by low levels of either ethanol or propanol, hence this result is not unexpected.<sup>26</sup> The entrapment of HSA into samples containing MTES resulted in improvements in the sensitivity of HSA to salicylate as the level of MTES increased, showing binding affinity which is apparently higher than that obtained in solution. Given that salicylate is relatively hydrophobic, the increased sensitivity to salicylate is likely the result of analyte preconcentration into these samples via a solid-phase extraction process. This behavior is useful for biosensor development since the sample of interest can be selectively extracted into the matrix, providing improved sensor performance.

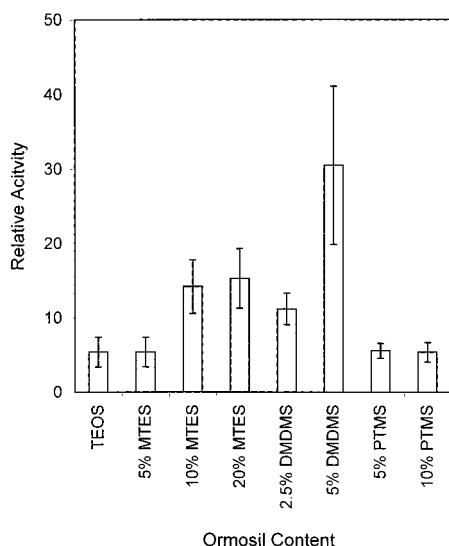


**Figure 9.** Relative activity of entrapped lipase as compared to the enzyme in solution.

*Lipase.* Figure 9 shows the percentage of activity for entrapped lipase samples as compared to the value in solution. In this case, entrapment of the protein into TEOS-derived samples results in almost complete loss of function, in agreement with the results of Reetz and co-workers.<sup>7a</sup> The presence of MTES results in an improvement in protein function which becomes greater as the level of MTES increases, and provides activity values that are ~3-fold higher than those obtained in TEOS-derived samples. The presence of PTMS resulted in no improvement in activity. This result was somewhat unexpected, and may be due to several factors, including enzyme denaturation, slow kinetics for diffusion of the analyte into or the product out of the matrix due to steric hindrance from the longer alkyl chains, or poor accessibility of the enzyme to the substrate. We are currently examining these possibilities and will report our findings in a future manuscript. The presence of DMDMS produced the highest activity levels for entrapped lipase, resulting in an activity value that was ~6-fold larger than that obtained in TEOS-derived samples. This result is interesting, given that MTES at twice the concentration, resulting in a similar number of methyl groups, did not provide as large an improvement in activity values. It is possible that the lower degree of cross-linking obtained with DMDMS may play a role in controlling the accessibility of analyte to the protein, and hence the apparent activity.

Overall, the ability to entrap lipase into optically clear hybrid materials with up to 30% retention of solution activity indicates that the development of an optical biosensor based on these biomaterials is possible. A wide variety of pH-sensitive fluorescent probes exist which could be coentrapped with lipase to produce a self-contained, "reagentless" sensor for triglycerides. Hydrolysis of the analyte to produce fatty acids should produce a fluorescence response which could then be

detected using a standard fiber-optic sensor format. We are currently working toward such a sensor in our laboratory and will report on the analytical performance of the device in a follow-up paper.

## Conclusions

The addition of specific organically modified silanes to sol-gel-derived materials formed primarily from TEOS can be used to control the polarity of the internal environment within the matrix. However, the range over which polarity can be controlled, without causing undesirable changes in the physical characteristics of the materials, is limited when using sol-gel preparation protocols which are suitable for protein encapsulation, and depends on the type of organosilane used. The addition of organically modified silanes to a matrix formed mainly from TEOS results in a decrease in hardness, optical clarity, and dehydration/rehydration stability and at high levels may cause phase separation. No significant differences in physical properties were detectable between samples made from cohydrolyzed silanes and those made from separately hydrolyzed silanes. However, the differences in the spectroscopic characteristics of both 7AI and prodan suggest that the internal environment of cohydrolyzed monoliths is more homogeneous than that of separately hydrolyzed monoliths, and that these distributions are affected by washing the monoliths after gelation. At low levels of organosilane, and particularly when MTES is used, it is possible to prepare optically transparent, durable, organic-inorganic hybrid materials. The results suggest that washed, cohydrolyzed silicates are likely to be optimal for development of useful sensor materials. Hence, such samples were used for protein entrapment studies. Both HSA and lipase were successfully entrapped into the hybrid materials with retention of structure and function. For HSA, it was possible to do fluorescence-based assays of ligand binding, showing the utility of the optically clear materials. For lipase, increased levels of ormosil, particularly DMDMS, produced improvements in protein activity, and the optical transparency allows spectroscopic assays of entrapped protein function to be done. The utility of these materials for optical sensor applications is currently being explored.

**Acknowledgment.** We wish to thank the Natural Sciences and Engineering Research Council of Canada and Research Corporation (Cottrell College Science Award to J.D.B.) for financial support. We also thank Mr. Tim Jones and Mr. James Shoemaker for technical assistance in acquiring NMR spectra.

**Supporting Information Available:** One table of NMR chemical shifts and four tables of fluorescence emission wavelength data. This material is available free of charge via the Internet at <http://pubs.acs.org>.

CM9910097